Stability of a Fermi ball against deformation from spherical shape

T. Yoshida
Department of Physics, Tokyo University, Hongo 7-3-1, Bunkyo-Ku, Tokyo 113-0033, Japan

K. Ogure
Department of Physics, Kobe University, Rokkoudaicho 1-1, Nada-Ku, Kobe 667-8501, Japan

J. Arafune
National Institution for Academic Degrees, Hitotsubashi 2-1-2, Chiyoda-Ku, Tokyo 101-8438, Japan
(Received 29 September 2002; published 23 April 2003)

The stability of a Fermi ball (F ball), which is a kind of nontopological soliton accompanying the breakdown of the approximate Z_2 symmetry, is investigated in three situations: when it is electrically neutral, when it is electrically charged and unscreened, and when it is electrically charged and screened. We argue only that the third case is physically meaningful since the neutral F ball is unstable and the case of an unscreened charged F ball is observationally excluded when it has a sizable contribution to CDM. We find that the energy scale of the breakdown of the approximate Z_2 symmetry v should satisfy $v<3\times10^6$ GeV if the F ball is the main component of CDM.

DOI: 10.1103/PhysRevD.67.083506 PACS number(s): 05.45.Yv, 95.35.+d

I. INTRODUCTION

An F ball, a kind of nontopological soliton, was introduced as a candidate for cold dark matter (CDM) [1,2]. A similar object is also suggested to play an important role in baryogenesis [3].

The simplest type of the F ball is a bubble of false vacuum surrounded by a thin domain wall on which many zero-mode fermions are attached. The surface tension of the wall is balanced with the Fermi pressure due to the zero-mode fermions in the wall. The F ball may be stabilized owing to this balance between the surface energy and the Fermi energy. Though the F ball is stable against the variation of the radius in case it keeps a spherical shape, it may be unstable against deformation from the sphere. Macpherson and Campbell pointed out in their pioneering work [1] that such F balls are unstable against deformation from the spherical shape, and that they should finally fragment into a number of tiny F balls [4] (see Fig. 1 for an illustration of a fragmenting F ball). Suppose there are a large number of such tiny F balls in the present universe contributing sizably to CDM. The cosmic flux of these objects should be large, proportional to the inverse of the mass, and they should have been observed contrary to the experimental results unless the scattering cross section with ordinary matter is very small. Here, we are not interested in such a new kind of weakly interacting particles since we need too many assumptions in introducing new tiny particles and have only an indirect means to detect such particles [1].

Morris then introduced the idea of an electrically charged F ball [5] which is considered to be stabilized due to the repulsive long-range Coulomb force [2]. Since the charged F balls can be large and heavy in this case, they can sizably contribute to CDM without contradicting the present observations of the cosmic flux. These F balls with a large cross section of interaction with ordinary matter are interesting because of their future detectability. [We nevertheless note that the cross section per unit mass for the F ball σ/M_f is not as large as the one which was recently proposed [6,7] for the self-interacting dark matter. We do not go into details since the above issue is still controversial (see the discussions in Sec. VI).]

In the present paper we first examine the instability of the neutral F ball against the deformation from the spherical shape. It is known [1] that the spherical shape is unstable against deformation due to the finite volume energy within the thin-wall approximation. We investigate the next-to-leading order approximation, the curvature effect of the wall, since it has a shape-dependent contribution to the total energy, and is important when the volume energy is very small. We find that the neutral F ball is unstable even in the presence of the curvature effect.

We next examine whether the F ball is stable when it is electrically charged and unscreened. Since the total energy of such an F ball is higher than the sum of the energies of the fragmented F balls, it fragments into smaller F balls in finite time. Its lifetime is, however, longer than the age of the universe if there is an energy barrier high enough between the state of an F ball and that of fragmented F balls. We see that the Coulomb force does make the lifetime of the F ball long enough.

We thirdly examine whether the F ball has a lifetime long enough to survive until present if it is screened due to the electrons or positrons in the thermal bath of the early uni-

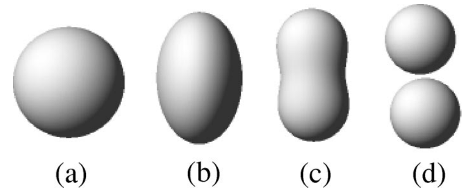

FIG. 1. A deformation and a fragmentation of the F ball. (a) Sphere. (b) Cigarlike deformation. (c) Shape narrow in the middle. (d) Fragmented F balls.

verse. Though the long-ranged Coulomb force becomes short ranged in the thermal bath, the lifetime of the F ball is found long enough in the proper region of the parameters.

We finally examine which kind of F balls satisfy the conditions for a main component of CDM. We find that only the screened F ball meets the conditions after taking into account the stability of the F ball, observational constraints, and cosmological considerations.

We focus on the Fermi ball in which the fermions are tightly bound in the domain wall and distribute only two dimensionally in the present paper. The effect of the distribution normal to the domain wall must be included in the case where they distribute with the thickness comparable to that of the domain wall. This effect is investigated elsewhere [8].

The above contents are organized as follows: We first consider electrically neutral F balls and discuss their stability in Sec. II. Small F balls which are electrically charged and not screened by electrons are considered in Sec. III. Screened ones are considered in Sec. IV; this is the main theme in the present paper. In Sec. V we discuss certain constraints on the parameters obtained from various conditions. We have summaries and discussions in Sec. VI. The detailed calculations are given in the Appendixes.

II. STABILITY OF AN ELECTRICALLY NEUTRAL F BALL

We briefly introduce the electrically neutral F ball proposed by Macpherson and Campbell [1] to make clear the notations and technical terms. The Lagrangian density is given by

$$\mathcal{L}=\frac{1}{2}(\partial_\mu\phi)^2+\overline{\psi_f}(i\gamma^\mu\partial_\mu-G\phi)\psi_f-U(\phi), \tag{1}$$

where ϕ and ψ_f are a scalar and a fermion field, respectively, and G is a Yukawa coupling constant. Here, $U(\phi)$ is an approximate double-well potential [9],

$$U(\phi)=\frac{\lambda}{8}(\phi^2-v^2)^2+U_\epsilon(\phi). \tag{2}$$

The first term has the Z_2 symmetry under $\phi\leftrightarrow-\phi$, and the second term violates the symmetry, though we assume it is much smaller than the first one (see Fig. 2). Thus, the Lagrangian density has an approximate Z_2 symmetry, which we call "biased Z_2 symmetry" [1] hereafter. Since we consider the case where the fermions are tightly bound in the domain wall, we assume that the coupling constants satisfy the condition $G\gg\sqrt{\lambda}$.

After the phase transition breaks spontaneously the biased Z_2 symmetry at $T=T_{ph}\sim v$, there arise two almost degenerate vacua with the energy density difference of ϵ. They are the true vacuum with $\phi=v$ and the false one with $\phi=-v$. Then a domain wall is produced between two vacua, and the fermions are captured as zero modes in the domain wall [10]. Though the effect of ϵ should be negligible soon after the phase transition, it gets more important as the universe expands. If the volume energy becomes larger than the surface energy during the expansion, the true vacuum is energetically favored and enlarges its volume. At the same time, the region of false vacuum gets diminished, and becomes a small confined region surrounded by the domain wall. Such a region of false vacuum would continue to shrink due to the surface tension and the volume effect proportional to ϵ, and finally disappear if we neglect the Fermi pressure caused by the zero-mode fermions trapped in the wall. In our case, however, the Fermi pressure is not negligible and stops the shrinkage of the region, when it gets balanced with the surface tension. Such a bubble of the false vacuum with zero-mode fermions trapped in the surrounding wall is called F ball [1]. We take the temperature for the F ball production as $T=T_f$. Because T_f is somewhat lower than T_{ph}, T_f is assumed to be $T_f\lesssim 0.1v$ in the present paper.

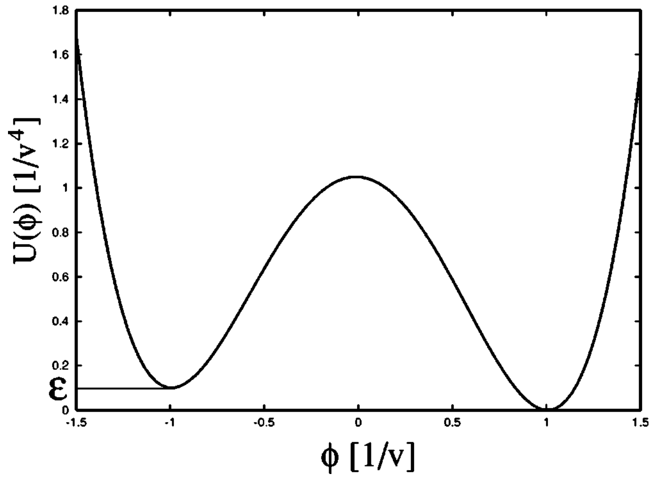

FIG. 2. The biased potential for $\lambda=1$. Two almost degenerate vacua with the energy difference of ϵ exist: the true vacuum with $\phi=v$ and the false vacuum with $\phi=-v$.

We consider a thin-walled F ball, the size of which is much larger than the thickness of the domain wall. For simplicity, we neglect the small energy difference ϵ and take the exact Z_2 symmetry until Sec. V. Then the Lagrangian density is

$$\mathcal{L}=\frac{1}{2}(\partial_\mu\phi)^2+\overline{\psi_f}(i\gamma^\mu\partial_\mu-G\phi)\psi_f-\frac{\lambda}{8}(\phi^2-v^2)^2. \tag{3}$$

The total energy of an F ball is expressed as

$$E_{tot}=E_s+E_f, \tag{4}$$

where E_s and E_f are a contribution from the domain wall and that from the zero-mode fermions, respectively. In the thin wall case, Fermi gas in the wall distributes two dimensionally on the surface of the F ball [11]. Taking the w axis normal to the surface, which is positive (negative) for the outside (inside) of the F ball, we express the fermion number density as

$$n_f=\sigma_f\delta(w), \tag{5}$$

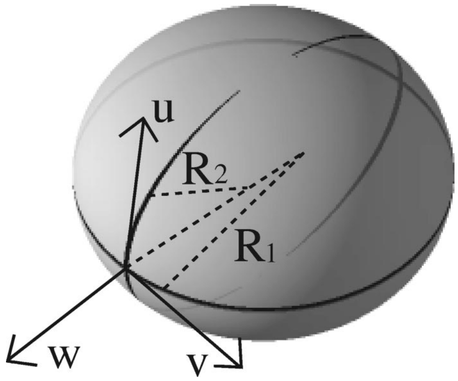

FIG. 3. The local orthogonal coordinates (u,v,w), the origin of which is on the surface of the F ball. We take u and v along the lines of curvature on the surface, and w normal to the surface. Here, R_1 (R_2) is a radius of principal curvature with respect to $u=0$ ($v=0$) at the origin.

with σ_f the surface density of the fermion number, and the Fermi energy

$$E_f=\frac{4\sqrt{\pi}}{3}\int \mathrm{d}S \quad \sigma_f^{3/2}. \tag{6}$$

We obtain the surface energy

$$E_s=\int \mathrm{d}S\mathrm{d}w \left|\left(1+\frac{w}{R_1}\right)\left(1+\frac{w}{R_2}\right)\right| \times\left\{\frac{1}{2}(\nabla\phi)^2+\frac{\lambda}{8}(\phi^2-v^2)^2\right\}, \tag{7}$$

where R_1 and R_2 are the radii of principal curvature of the F-ball surface (see Fig. 3 and Appendix A).

If the fermion-scalar coupling G is not too small, the F ball is stable against releasing a fermion with mass $\sim Gv$ from the wall to the vacuum. The number of the fermions of the F ball,

$$N_f=\int \mathrm{d}S \quad \sigma_f, \tag{8}$$

is then conserved. Thus, the energy of the F ball is obtained by minimizing

$$E_{tot;\mu}=E_{tot}+\mu\left(N_f-\int \mathrm{d}S \quad \sigma_f\right), \tag{9}$$

with μ the Lagrange multiplier. We first minimize it with respect to σ_f. Noting that E_s is independent of σ_f, we obtain the uniform distribution of the fermions,

$$\sigma_f=\frac{N_f}{S}, \tag{10}$$

with S the area of the F-ball surface. We next minimize the energy with respect to ϕ. Assuming that the variation of ϕ in the direction parallel to the F-ball surface is much smaller than that in the direction w, we get the Euler-Lagrange equation for ϕ,

$$\ddot{\phi}+\left(\frac{1}{R_1+w}+\frac{1}{R_2+w}\right)\dot{\phi}=\frac{\lambda}{2}\phi(\phi^2-v^2), \tag{11}$$

with the overdot symbol in $\dot{\phi}$ or $\ddot{\phi}$ standing for the derivative with respect to w. Here, ϕ fulfills the boundary condition,

$$\phi=\begin{cases} +v & (w\gg\delta_n), \\ 0 & (w=0), \\ -v & (w\ll-\delta_n), \end{cases} \tag{12}$$

with δ_n the width of the wall. We take the leading contribution, ϕ_0, in the thin-wall expansion with $R_1,R_2\to\infty$. It satisfies

$$\ddot{\phi}_0=\frac{\lambda}{2}\phi_0(\phi_0^2-v^2), \tag{13}$$

with

$$\phi_0=\begin{cases} +v & (w\gg\delta_n), \\ 0 & (w=0), \\ -v & (w\ll-\delta_n). \end{cases} \tag{14}$$

The solution for ϕ_0,

$$\phi_0=v\tanh\frac{w}{\delta_n}, \tag{15}$$

with $\delta_n=2/(\sqrt{\lambda}v)$, minimizes the energy under the condition, Eq. (10), to be

$$E_{tot}^{(0)}=\Sigma S+\frac{4\sqrt{\pi}N_f^{3/2}}{3\sqrt{S}}, \tag{16}$$

with $\Sigma=2\sqrt{\lambda}v^3/3$ the surface tension in the wall. We finally minimize $E_{tot}^{(0)}$ with respect to S, and obtain

$$E_{tot}^{(0)}=(12\pi\Sigma)^{1/3}N_f, \tag{17}$$

with the area of the surface, $S=(2\sqrt{\pi}/3\Sigma)^{2/3}N_f$. An F ball can deform with this surface area being kept constant [see Figs. 1(a)–1(c)]. Moreover, it has the same energy even if it splits into some smaller F balls [see Fig. 1(d)] since $E_{tot}^{(0)}$ is proportional to the number of fermions. Thus, we cannot tell whether the F ball is stable or not against deformation and fragmentation into pieces, within the thin-wall approximation which corresponds to the leading order in the thin-wall expansion. This is the same result as what Macpherson and Campbell derived in their paper [1]. They concluded further that the neutral F ball is unstable, taking into account the volume effect proportional to ϵ. We here consider the next-to-leading order contribution in the thin-wall expansion, i.e.,

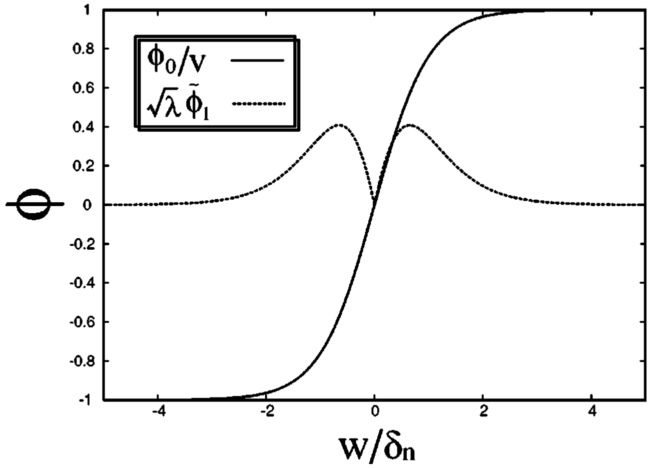

FIG. 4. The perturbative solutions for the domain wall field ϕ. Here, ϕ_0 is the leading term and ϕ_1 the next-to-leading term in the thin-wall expansion. Note that ϕ_0 is rescaled as ϕ_0/v with v the symmetry breaking scale, and ϕ_1 as $\sqrt{\lambda}\tilde{\phi}_1$ with $\tilde{\phi}_1 = 2R_1R_2\phi_1/(R_1+R_2)$ (R_1 and R_2 are the radii of principal curvature of the F-ball surface).

the curvature effect, since such an effect becomes important when it is comparable to the volume energy effect.

We keep the terms up to the next-to-leading order for ϕ,

$$\phi = \phi_0 + \phi_1, \tag{18}$$

with ϕ_1 smaller than ϕ_0 by the order of δ_n/R [12]. From Eqs. (11) and (12), ϕ_1 satisfies

$$\ddot{\phi}_1 - \frac{\lambda}{2}(3\phi_0^2 - v^2)\phi_1 = -\left(\frac{1}{R_1}+\frac{1}{R_2}\right)\dot{\phi}_0, \tag{19}$$

and the boundary condition

$$\phi_1 = \begin{cases} 0 & (|w| \gg \delta_n), \\ 0 & (w=0). \end{cases} \tag{20}$$

The analytic solution [13] for ϕ_1 is given in Appendix B (see Fig. 4 for the illustration of ϕ_0 and ϕ_1). Substituting the solution for ϕ_1 and that for ϕ_0 into E_{tot} and keeping the terms up to the order of $O((\delta_n/R)^2 E_{tot}^{(0)})$ [14], we get (see Appendix B)

$$E_{tot} = E_{tot}^{(0)} + E_{tot}^{(2)}, \tag{21}$$

where

$$E_{tot}^{(2)} = C_n \int \mathrm{d}S \ \frac{1}{|R_1R_2|} + D_n \int \mathrm{d}S \ \left(\frac{1}{R_1}-\frac{1}{R_2}\right)^2 \frac{|R_1R_2|}{R_1R_2}. \tag{22}$$

Here, C_n and D_n are given by

$$C_n = \int \mathrm{d}w \ \ (w^2\dot{\phi}_0{}^2 - \dot{\phi}_0\tilde{\phi}_1)$$

$$\simeq -\frac{0.25v}{\sqrt{\lambda}}, \tag{23}$$

$$D_n = -\frac{1}{4}\int \mathrm{d}w \ \ \dot{\phi}_0\tilde{\phi}_1$$

$$\simeq -\frac{0.28v}{\sqrt{\lambda}}, \tag{24}$$

with $\tilde{\phi}_1 = 2R_1R_2\phi_1/(R_1+R_2)$.

First, we examine the stability of the spherical F ball against the perturbative deformation from the spherical shape [see Fig. 1(b)]. For this purpose, we take the curvature radius on the F-ball surface positive. In this case, the first term in Eq. (22) is constant according to the Gauss-Bonnet theorem [15]. Thus, the shape-dependent sector in E_{tot} comes from the second term in Eq. (22). Because it is semi-negative definite, and zero only for the spherical shape, the spherical F ball is unstable against the perturbative deformation.

We next consider the stability of the F-ball against fragmentation into smaller ones (see Fig. 1(d)). In this case, the fragmentation does not change $E_{tot}^{(0)}$ because it only depends on the fermion number. Here, we compare the energy of the spherical F ball with that of the fragmented spherical F balls for simplicity. We see that the second term in Eq. (22) vanishes. Thus, only the first term in Eq. (22) changes in the fragmentation. Since it is proportional to the number of F balls due to the Gauss-Bonnet theorem, its negative sign shows that the fragmentation is energetically promoted. Therefore, we find that the F ball is unstable against not only the deformation from the spherical shape but also the fragmentation into smaller ones.

As pointed out by Macpherson and Campbell, the fragmentation will continue until the thin-wall expansion gets invalid. If the fragmented tiny F balls sizably contribute to CDM, there should be a large number of them and a large cosmic flux of them as well. The present observations for the dark matter search tell that they can interact with ordinary matter only very weakly. Such F balls are not considered here since their detectability was discussed in Ref. [1].

III. STABILITY OF ELECTRICALLY CHARGED *F* BALL IN THE UNSCREENED CASE

In the present section we consider the electrically charged F ball proposed by Morris [2], in which the fermions trapped on the surface have electric charge. Assigning the electric charge of $+e$ to the fermion for simplicity, we consider an F ball carrying the electric charge $+eN_f$. The energy of the F ball is expressed as

$$E_{tot} = E_s + E_f + E_c, \tag{25}$$

with E_c the Coulomb potential energy. Since the Coulomb energy is proportional to the fermion number squared E_c

$\propto N_f^2$, the total energy per unit fermion number E_{tot}/N_f is an increasing function of N_f. Thus, when the F ball fragments into smaller ones, the total energy apparently decreases. We therefore cannot conclude that the electric force stabilizes the F ball from fragmentation only by comparing the energies of the two states. Morris, however, suggested [2] that the inclusion of the long ranged repulsive force helps the F ball to be stabilized. Since it is not so clear whether the electric repulsive force stabilizes the F ball or not, we here verify it using the perturbative method.

For this purpose we investigate whether the energy barrier exists between the F ball before the fragmentation and that after it. Let us consider a spherical F ball and its perturbative deformation from the spherical shape. Assuming the rotational invariance around the z axis for simplicity, we express the surface of the F ball in the polar coordinates as

$$\mathbf{x}_f(\theta,\varphi)=r(\theta)\mathbf{e}, \tag{26}$$

with $\mathbf{e}$ a unit vector,

$$\mathbf{e}=(\sin\theta\cos\varphi,\sin\theta\sin\varphi,\cos\theta). \tag{27}$$

We expand $r(\theta)$ as

$$r(\theta)=R\left(1+\sum_{l=1}^{\infty}a_l P_l(\cos\theta)\right)$$
$$\equiv R(1+\delta r), \tag{28}$$

where a_l's are small coefficients of the perturbative expansion, and $P_l(\cos\theta)$ is the Legendre polynomial. We write the surface element as

$$\mathrm{d}S=R^2(1+\delta S(a_l))\mathrm{d}\Omega, \tag{29}$$

with $\mathrm{d}\Omega=\sin\theta\,\mathrm{d}\theta\mathrm{d}\varphi$. We also expand the surface density of the fermion as

$$\sigma_f(\theta)=\frac{N_f}{4\pi R^2(1+\delta S)}\left(1+\sum_{l=1}^{\infty}c_l P_l(\cos\theta)\right)$$
$$\equiv\frac{N_f}{4\pi R^2(1+\delta S)}(1+\delta\sigma_f), \tag{30}$$

where c_l's are small expansion coefficients. Note that the above expression satisfies the condition for the fermion number N_f to be conserved [see Eq. (8)].

Keeping the terms up to the second power of a_l and c_l (see Appendix C), we estimate, within the thin-wall approximation, the surface energy

$$E_s=\Sigma S=4\pi\Sigma R^2\left(1+\sum_{l=1}^{\infty}\frac{h_s^{(l)}}{2l+1}\right), \tag{31}$$

the Fermi energy

$$E_f=\frac{4\sqrt{\pi}}{3}\int\mathrm{d}S\ \ \sigma_f^{3/2}=\frac{2N_f^{3/2}}{3R}\left(1+\sum_{l=1}^{\infty}\frac{h_f^{(l)}}{2l+1}\right), \tag{32}$$

and the Coulomb potential energy

$$E_c=\frac{e^2}{8\pi}\int\int\mathrm{d}S\mathrm{d}S'\ \frac{\sigma_f\sigma_f'}{|\mathbf{x}_f-\mathbf{x}_f'|}=\frac{e^2N_f^2}{8\pi R}\left(1+\sum_{l=1}^{\infty}\frac{h_c^{(l)}}{2l+1}\right), \tag{33}$$

where

$$h_s^{(l)}=\left(1+\frac{l(l+1)}{2}\right)a_l^2, \tag{34}$$

$$h_f^{(l)}=-\frac{1}{2}\left(1+\frac{l(l+1)}{2}\right)a_l^2+\frac{3}{8}b_l^2, \tag{35}$$

$$h_c^{(l)}=-\frac{l^2+3l-1}{2l+1}a_l^2-\frac{2(l-1)}{2l+1}a_lb_l+\frac{1}{2l+1}b_l^2, \tag{36}$$

with $b_l=c_l-2a_l$. Using the effective radius

$$R_e\equiv\sqrt{\frac{S}{4\pi}}=R\left(1+\frac{1}{2}\sum_{l=1}^{\infty}\frac{h_s^{(l)}}{2l+1}\right), \tag{37}$$

we express the total energy as

$$E_{tot}=4\pi\Sigma R_e^2+\frac{2N_f^{3/2}}{3R_e}\left(1+\sum_{l=1}^{\infty}\frac{g_f^{(l)}}{2l+1}\right)$$
$$+\frac{e^2N_f^2}{8\pi R_e}\left(1+\sum_{l=1}^{\infty}\frac{g_c^{(l)}}{2l+1}\right), \tag{38}$$

where

$$g_f^{(l)}=\frac{3}{8}b_l^2, \tag{39}$$

$$g_c^{(l)}=(l-1)\left(-\frac{3}{2(2l+1)}+\frac{l}{4}\right)a_l^2-\frac{2(l-1)}{2l+1}a_lb_l+\frac{b_l^2}{2l+1}. \tag{40}$$

Minimizing E_{tot} with respect to R_e, we have

$$E_{tot}=(12\pi\Sigma)^{1/3}N_f\left(1+\frac{3e^2\sqrt{N_f}}{16\pi}\right)^{2/3}\left\{1+\frac{2}{3\left(1+\frac{3e^2\sqrt{N_f}}{16\pi}\right)}\times\sum_{l=1}^{\infty}\frac{1}{2l+1}\left(g_f^{(l)}+\frac{3e^2\sqrt{N_f}}{16\pi}g_c^{(l)}\right)\right\}, \tag{41}$$

with the effective radius

$$R_e=\frac{\sqrt{N_f}}{(12\pi\Sigma)^{1/3}}\left(1+\frac{3e^2\sqrt{N_f}}{16\pi}\right)^{1/3}\left\{1+\frac{1}{3\left(1+\frac{3e^2\sqrt{N_f}}{16\pi}\right)}\times\sum_{l=1}^{\infty}\frac{1}{2l+1}\left(g_f^{(l)}+\frac{3e^2\sqrt{N_f}}{16\pi}g_c^{(l)}\right)\right\}. \tag{42}$$

Since the last term in the brackets { } in Eq. (41) is semipositive definite and zero only for $b_1=0$ and $a_l=b_l=0$ for $l\geqslant 2$, E_{tot} takes the local minimum when the F ball is spherical (we note that the parameter a_1 corresponds to the small parallel displacement and not to the deformation of the F ball). Thus, the spherical F ball is stable against the perturbative deformation from the spherical shape. It leads to the existence of the energy barrier and should suppress the fragmentation of the spherical F ball. If the suppression of the fragmentation rate is strong, the F balls would be effectively stable in the universe (for the detailed discussion on their lifetime, see Appendix D) and could be the candidates for CDM. However, if N_f is very large, the F ball should have such a strong electric field that should be quantum-mechanically screened by electrons or positrons with the screening length much shorter than the F-ball radius, as we see in the next section. Therefore, the argument of this section cannot be applied for the F ball with very large N_f.

The argument of this section is applicable only for the F balls with small N_f, which have the radius much smaller than the screening length. Such F balls should give too large cosmic flux to be compatible with the present observations if the F balls contribute sizably to CDM (the more details are given in Sec. V and Ref. [16]). We therefore find that the unscreened charged F ball cannot be a main component of CDM.

IV. STABILITY OF AN ELECTRICALLY CHARGED F BALL IN THE SCREENED CASE

In this section we examine the stability of such a large F ball that is electrically charged and screened due to the electrons produced quantum mechanically or thermally. We call the fermion trapped on the F-ball surface a ‘‘heavy fermion’’ in order to distinguish it from the electron; the heavy fermion is almost massless in the two-dimensional surface while it is as heavy as Gv in the true vacuum. The property of the screened F ball is quite different from that of an unscreened one, because the long ranged electric force becomes short ranged as a result of the screening. Let us investigate the screening effect by introducing the Coulomb potential energy V_e for electron ($-V_e$ for positron) with $V_e=-eA_0$. We use the Thomas-Fermi method [17,18] to deal with this problem [19]. The Helmholtz free energy is expressed as

$$F_{tot}=F_n+F_{sc}, \tag{43}$$

where F_n is the non-Coulombic term that is the same as the energy for the neutral F ball (see Sec. II). The second term F_{sc} is the contribution from the screening electrons,

$$F_{sc}=\int \mathrm{d}S\mathrm{d}w \; \left|\left(1+\frac{w}{R_1}\right)\left(1+\frac{w}{R_2}\right)\right| \times\left\{-\frac{1}{2e^2}(\nabla V_e)^2+\mathcal{F}_e-n_fV_e\right\}, \tag{44}$$

with $\mathcal{F}_e$ the free energy density of electron and positron in the Coulomb potential [20],

$$\mathcal{F}_e=-\frac{2T}{(2\pi)^3}\int \mathrm{d}^3\mathbf{p}\;\{\log(1+e^{-(E-V_e)/T}) +\log(1+e^{-(E+V_e)/T})\}. \tag{45}$$

Here, the kinetic energy E is given by $E=\sqrt{\mathbf{p}^2+m_e^2}$ with m_e the electron mass, and the density of the heavy fermion n_f is given by $n_f=\sigma_f\delta(w)$. [Note that the negative sign of the first term in { } in Eq. (44) gives the correct electric energy density, $+\mathbf{E}^2/2$, after the free energy is extremized with respect to V_e.] Taking into account the conservation of the heavy fermion number, we obtain the free energy by extremizing $F_{tot}+\mu(N_f-\int \mathrm{d}S\;\sigma_f)$ with respect to ϕ, σ_f, and V_e. The procedure of extremization with respect to ϕ and σ_f is the same as in Sec. II, and we refer to the discussions and results there.

Now let us extremize the free energy with respect to V_e. Assuming that the variation of V_e in the direction parallel to the F-ball surface is much smaller than that in the normal direction, we get the Thomas-Fermi equation

$$\frac{1}{e^2}\ddot{V}_e+\frac{1}{e^2}\left(\frac{1}{R_1+w}+\frac{1}{R_2+w}\right)\dot{V}_e=n_f(w)-\overline{n}_e(w), \tag{46}$$

where the overdot symbol stands for the partial derivative with respect to w. Here, $\overline{n}_e(w)=\partial\mathcal{F}_e/\partial V_e$ is the expectation value of the difference between the electron density and the positron density. The second term in the left-hand side (lhs) in Eq. (46) comes from the curvature effect, which was not taken into account in the previous works. We here impose the boundary condition

$$V_e\to 0 \quad \text{for} \;\; |w|\gg\delta_{sc}, \tag{47}$$

with δ_{sc} the typical screening length. For the case, $T\gg m_e$, the electron number density is expressed as

$$\overline{n}_e\simeq-\frac{T^2V_e}{6}-\frac{V_e^3}{3\pi^2}. \tag{48}$$

Note that $\overline{n}_e$ is positive since we take V_e negative, assuming the F ball carrying the positive electric charge. In the first place, let us obtain the leading contribution in the thin-wall expansion by taking $R_1,R_2\to\infty$. We get

$$V_e^{(0)}=\frac{-\sqrt{2}\pi T}{\sinh\left(\frac{|w|+\delta_{sc}}{\lambda_T}\right)}, \tag{49}$$

where

$$\lambda_T = \frac{\sqrt{3}}{eT}, \tag{50}$$

$$\delta_{sc} = \lambda_T \cosh^{-1} \frac{\sqrt{2}\pi T^2 + \sqrt{2\pi^2 T^4 + 3e^2\sigma_f^2}}{\sqrt{3}e\sigma_f},$$

$$\simeq \sqrt{\frac{2\sqrt{6}\pi}{e^3\sigma_f}} \quad (v \gg T). \tag{51}$$

Substituting $V_e^{(0)}$ into F_{sc} and keeping the terms of the leading order, we get the leading order of F_{sc} as

$$\begin{aligned} F_{sc}^{(0)} &= \int dS \int dw \left\{ -\frac{1}{2e^2}\dot{V}_0^2 - \frac{T^2 V_0^2}{6} \right. \\ &\quad \left. - \frac{V_0^4}{12\pi^2} - \sigma_f V_0 \delta(w) \right\} \\ &= \frac{8\pi^2 T^3}{\sqrt{3}e} \int dS \left\{ \coth^3\left(\frac{\delta_{sc}}{\lambda_T}\right) - \frac{3}{2}\coth\left(\frac{\delta_{sc}}{\lambda_T}\right) + \frac{1}{2} \right\} \\ &\simeq \sqrt{\frac{2\sqrt{2}\pi e}{3\sqrt{3}}} \int dS \sigma_f^{3/2} \quad (v \gg T). \end{aligned} \tag{52}$$

From the above equation, we see that the heavy fermions distribute uniformly over the surface, as is the case with Eq. (10). Then, $\phi^{(0)}$ in Eq. (15) and $V_e^{(0)}$ in Eq. (49) extremize the free energy,

$$F_{tot}^{(0)} = \Sigma S + \left(\frac{4\sqrt{\pi}}{3} + \sqrt{\frac{2\sqrt{2}\pi e}{3\sqrt{3}}} \right) \frac{N_f^{3/2}}{\sqrt{S}}. \tag{53}$$

Minimizing the free energy with respect to S, we obtain

$$F_{tot}^{(0)} = (12\pi\Sigma)^{1/3} \left(1 + \sqrt{\frac{\sqrt{3}e}{4\sqrt{2}}} \right)^{2/3} N_f, \tag{54}$$

with the surface area

$$S = \left(\frac{2\sqrt{\pi}}{3\Sigma} \right)^{2/3} \left(1 + \sqrt{\frac{\sqrt{3}e}{4\sqrt{2}}} \right)^{2/3} N_f. \tag{55}$$

Thus, we cannot tell, within the leading order of the thin-wall expansion, whether the F ball is stable against the classical deformation and fragmentation into smaller ones.

We then keep the terms up to the next-to-leading order in the thin-wall expansion to have

$$V_e = V_e^{(0)} + V_e^{(1)}, \tag{56}$$

with $V_e^{(1)}$ smaller than $V_e^{(0)}$ by the order of δ_{sc}/R [21]. From Eqs. (46) and (47), $V_e^{(1)}$ satisfies

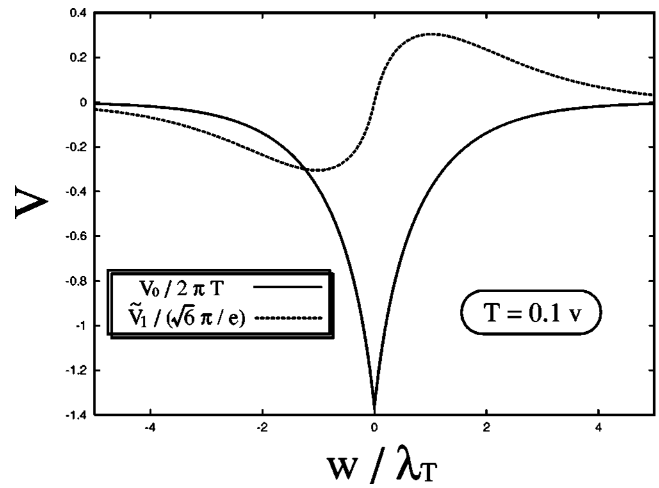

FIG. 5. The perturbative solutions for the electron potential energy V_e. Here, V_0 is the leading term and V_1 the next-to-leading term in the thin-wall expansion. Note that V_0 is rescaled as $V_0/2\pi T$ with T temperature, and V_1 as $e\tilde{V}_1/\sqrt{6}\pi$ with $\tilde{V}_1 = 2R_1R_2V_1/(R_1+R_2)$ (R_1 and R_2 are the radii of the principal curvature of the F-ball surface).

$$\frac{1}{e^2}\ddot{V}_e^{(1)} - \left(\frac{T^2}{3} + \frac{(V_e^{(0)})^2}{\pi^2} \right) V_e^{(1)} = -\frac{1}{e^2}\left(\frac{1}{R_1} + \frac{1}{R_2} \right) \dot{V}_e^{(0)}, \tag{57}$$

with the boundary condition

$$V_e^{(1)} \to 0 \quad \text{for } |w| \gg \delta_{sc}. \tag{58}$$

The solution to Eq. (57) is given by

$$\begin{aligned} V_e^{(1)} &= -\frac{\sqrt{6}\pi|w|}{2ew}\left(\frac{1}{R_1} + \frac{1}{R_2} \right) \frac{\cosh\left(\frac{|w|+\delta_{sc}}{\lambda_T}\right)}{\sinh^2\left(\frac{|w|+\delta_{sc}}{\lambda_T}\right)} \\ &\quad \times \left\{ f\left(\frac{|w|+\delta_{sc}}{\lambda_T}\right) - f\left(\frac{\delta_{sc}}{\lambda_T}\right) \right\}, \end{aligned} \tag{59}$$

where

$$f(x) \equiv \tfrac{1}{3}\sinh x \cosh x + \tfrac{2}{3}\tanh x - \tfrac{1}{3}\sinh^2 x - x \tag{60}$$

(see Fig. 5 for the illustration of $V_e^{(0)}$ and $V_e^{(1)}$). Substituting the solutions, $V_e^{(0)}$ and $V_e^{(1)}$, into F_{sc} and keeping the terms up to the next-to-leading order, we get, in a manner similar to the derivation of Eq. (21),

$$F_{sc} = F_{sc}^{(0)} + F_{sc}^{(2)}, \tag{61}$$

where [22]

$$F_{sc}^{(2)} = C_{sc}\int dS \frac{1}{|R_1R_2|} + D_{sc}\int dS \left(\frac{1}{R_1} - \frac{1}{R_2} \right)^2 \frac{|R_1R_2|}{R_1R_2}. \tag{62}$$

Here C_{sc} and D_{sc} are given by

$$C_{sc} = -\frac{1}{e^2}\int \mathrm{d}w \;\; \{w^2(\dot{V}_e^{(0)})^2 - \dot{V}_e^{(0)}\tilde{V}_e^{(1)}\}$$

$$\simeq -50\lambda^{1/6}v, \tag{63}$$

$$D_{sc} = \frac{1}{4e^2}\int \mathrm{d}w \;\; \dot{V}_e^{(0)}\tilde{V}_e^{(1)}$$

$$\simeq 25\lambda^{1/6}v, \tag{64}$$

with $\tilde{V}_e^{(1)} = 2R_1R_2V_e^{(1)}/(R_1+R_2)$. Note that D_{sc} is positive in contrast to the case with the neutral F ball where D_n in Eq. (24) is negative. This feature is very important for the discussion on the stability below. From Eqs. (22) and (62), we obtain

$$F_{tot}^{(2)} \simeq -\left(50\lambda^{1/6} + \frac{0.25}{\sqrt{\lambda}}\right)v\int \mathrm{d}S \;\; \frac{1}{|R_1R_2|} + \left(25\lambda^{1/6} - \frac{0.28}{\sqrt{\lambda}}\right)v\int \mathrm{d}S \;\; \left(\frac{1}{R_1} - \frac{1}{R_2}\right)^2 \frac{|R_1R_2|}{R_1R_2}. \tag{65}$$

Let us take the curvature radius of the F-ball surface positive, and consider the fragmentation of the spherical F ball into smaller F balls. The negative sign of the first term in Eq. (65) shows that the fragmentation is energetically promoted, which is the same as the neutral F ball in Sec. II. On the other hand, the sign of the second term is positive for

$$\lambda > 1.2\times 10^{-3}, \tag{66}$$

and there should be the energy barrier to suppress the fragmentation of the F ball. In this sense, electrically charged F balls which are screened by electrons are metastable [23] at $T \lesssim 0.1v$ (see the discussion in Appendix E).

The lifetime of the screened F ball is estimated in Appendix E and is found extremely long, which makes the F ball effectively stable. Thus, the screened charged F balls can be the candidates for CDM. In order for them to be a main component of CDM, they should satisfy the constraints to be discussed in the next section.

V. CONSTRAINTS ON THE PARAMETERS OF F-BALL

We consider the phase transition of the universe where the biased Z_2 symmetry is spontaneously broken and the network of domain walls is formed [24]. The number density of domain walls is soon diluted by annihilation to become $\sim 1/H^3$, where H is the Hubble constant. Using the energy density of the domain walls, $\rho_{wall} \sim \Sigma H$, we get the ratio of ρ_{wall} to the total energy density in the universe ρ_{tot},

$$\frac{\rho_{wall}}{\rho_{tot}} \simeq \frac{\Sigma H}{g_* T^4} \simeq \frac{\Sigma}{HM_{pl}^2}, \tag{67}$$

with g_* is the effective degree of freedom [25] and M_{pl} is the Planck mass. The ratio will be of the order of unity when $H \sim H_{eq} = \Sigma/M_{pl}^2$.

The small violation of the Z_2 symmetry gives an energy of the false vacuum bubble proportional to its volume. This volume energy increases with the universe expansion and gets comparable to the surface energy at $H \sim H_f = \epsilon/\Sigma$. The domain walls then stop to expand getting round to produce F balls. From the cosmological viewpoint, F balls should be produced before the domain walls dominate the total energy density in the universe, since otherwise the energy of the universe would be dominated by blackholes made with the domain walls [24]. This condition is $H_f > H_{eq}$, which is rewritten in terms of ϵ,

$$\epsilon > 0.4\lambda v^6 M_{pl}^{-2}. \tag{68}$$

Let us consider the case where the F balls are metastable and may contribute sizably to CDM in the present universe. As mentioned in Sec. II, we are not interested in the neutral F ball, which is very tiny after the fragmentations, since we need too many new assumptions in introducing such an object and have only indirect means to detect it. We thus consider the charged F balls. Since they interact with ordinary matter through the electric force, they would be easily observed in various experiments for the dark matter search if there exists enough cosmic flux. If the F ball has a considerable contribution to CDM, the number density and its cosmic flux should be inversely proportional to its mass, $1/M_f$. Since such events have not been observed so far, we should have $M_f > 10^{25}$ GeV [16]. This constraint is rewritten in terms of N_f,

$$N_f > 10^{25}\left(\frac{\mathrm{GeV}}{\lambda^{1/6}v}\right). \tag{69}$$

If the size of the F ball is smaller than the typical screening length, its electric charge is not screened at the close neighborhood of the F ball but screened far outside of it. In this case, the discussion on the stability made in Sec. III is valid. From Eqs. (42) and (51), we have the size of the unscreened F ball $R \sim 0.5\sqrt{N_f}(1+4/3\alpha\sqrt{N_f})^{1/3}/\lambda^{1/6}v$ and the screening length $\delta_{sc} \sim 30/\lambda^{1/6}v$, which gives a very small number of the fermion on the unscreened F ball, $N_f < 1000$, from $R < \delta_{sc}$. This is incompatible with Eq. (69), and we see that the unscreened F ball cannot give a sizable contribution to CDM.

If the size of the F ball is much larger than the screening length (i.e., $R \gg \delta_{sc}$), its electric charge is strongly screened as was discussed in the previous section. In this case, Eqs. (51) and (55) give $N_f \gg 7000$, which is compatible with Eq. (69). This allows screened charged F balls to be candidates for the main component of CDM in the present universe.

In the previous section we found that the second term in Eq. (65) is crucial to enhancing the stability and suppressing the fragmentation of the screened charged F ball for the parameter satisfying Eq. (66). If we add the volume energy $E_v \sim \epsilon V$ which has the destabilizing effect [26], we still have the metastable F ball as far as the second term in Eq. (65) overwhelms E_v. Using Eq. (64), we express this condition as

$$\epsilon < 100\lambda^{2/3} v^4 N_f^{-3/2}. \tag{70}$$

Equations (68)–(70) and Eq. (66) give the following condition for the symmetry breaking scale:

$$v < 3\times 10^6 \ \ \mathrm{GeV}. \tag{71}$$

VI. SUMMARY AND DISCUSSION

We have considered the F balls produced in the early universe due to the spontaneous breakdown of the biased Z_2 symmetry. We have investigated the stability of the electrically neutral F balls and the charged F balls in order to examine whether they can sizably contribute to CDM or not.

In the case of neutral F balls, we have taken into account the correction to the thin-wall approximation up to the next-to-leading order, and found this correction plays an important role to enhance deformation and fragmentation of the F ball into tiny thick-wall F balls. If these tiny F balls are a main component of CDM, the dark matter search experiments allow the F ball to have only a weak interaction with the ordinary matter. We are not interested in such a new kind of weakly interacting particles since we need too many new assumptions in introducing new tiny particles and have only indirect means to detect such particles [1].

In the case of charged F balls, two cases are considered:

Case (1). The size of a charged F ball being smaller than the typical screening length. Such F balls are found to have rather light masses, and they have a large number density in the universe if they are a main component of CDM. However, since the cosmic flux and the number density of the charged F balls are observed to be very small, it is difficult for them to be a main component of CDM. (In this case, the electric charge of the F balls is effectively unscreened. We have found that they decay into smaller F balls through the tunneling effect though they are classically stable. Since this decay further increases the large number density of the F balls, it merely decreases the possibility for them to be a main component of CDM.)

Case (2). The size of a charged F ball being larger than the typical screening length. In this case, the electric charge of the F ball is screened in the vicinity of its surface. Even though the long-range character of the Coulomb force is lost, the F balls can still be classically stable in certain region of the parameters. This is due to the curvature effect that is obtained from the next-to-leading order correction to the thin-wall approximation. Such F balls can be candidates for a main part of CDM in the present universe. In such a case, we have obtained constraints on the physical parameters: $\lambda > 1.2\times 10^{-3}$, $0.4\lambda v^6 M_{pl}^{-2} < \epsilon < 100\lambda^{2/3} v^4 N_f^{-3/2}$ and $v < 3\times 10^6$ GeV. It is interesting to note that the symmetry breaking scale v constrained above is not too far from the electroweak or supersymmetry (SUSY) breaking scale. These above constraints help us to make a realistic model of the F ball.

Recently the dark matter distributions of galaxies and clusters were observed and compared with the dark matter simulations. Some find consistency of the collisionless CDM simulation with the observations [27,28], while others find inconsistency and propose [6] the self-interacting dark matter (SIDM) with the ratio of the cross section to the mass as large as $10^{-23}-10^{-24}$ cm^2 GeV^{-1}. In the case of a screened charged F ball, the geometrical cross section per unit mass is not so large,

$$\frac{\sigma_g}{M_f} \simeq 0.5\lambda^{-1/2}\times 10^{-28}\left(\frac{\mathrm{GeV}}{v}\right)^3 \ \mathrm{cm}^2\,\mathrm{GeV}^{-1}, \tag{72}$$

and, moreover, the typical momentum transfer squared $\sim 1/R^2 \sim v^2/N_f$ is too small to give a large angle scattering which appears to be necessary for smoothing the Halo central density profile. Thus, the present model of the F ball is not adequate for SIDM. We, however, do not discuss this issue further in the present paper since the above problem is still controversial [7,27,29].

All through the present paper, we have dealt with the heavy fermions as being distributed two dimensionally on the F-ball surface, and neglected the spreading of the fermion in the direction normal to the surface. We discuss this issue elsewhere [8].

ACKNOWLEDGMENTS

We are grateful to Makoto Sakamoto, Masahiro Kawasaki, Shigeki Matsumoto, Masahide Yamaguchi, and Masamune Oguri for useful comments. We would like to thank Kojin Takeda and Hisaki Hatanaka for helpful conversations. One of the authors (K.O.) acknowledges financial support from Japan Society for Promotion of Science (No. 4834).

APPENDIX A: VOLUME ELEMENT IN NEW COORDINATES

We introduce three local orthogonal coordinates (u,v,w) for the F ball, the origin of which is on the surface of an F ball, and derive a representation for the volume element in this frame. The coordinates, u and v, represent the F-ball surface, $\mathbf{x}=\mathbf{x}_f(u,v)$, and are taken along the lines of curvature [30] on the surface. We define the first and the second fundamental forms

$$I = E(u,v)\mathrm{d}u^2 + 2F(u,v)\mathrm{d}u\,\mathrm{d}v + G(u,v)\mathrm{d}v^2, \tag{A1}$$

$$J = L(u,v)\mathrm{d}u^2 + 2M(u,v)\mathrm{d}u\,\mathrm{d}v + N(u,v)\mathrm{d}v^2, \tag{A2}$$

with the coefficients

$$\begin{aligned} E(u,v) &= \mathbf{x}_{f,u}\mathbf{x}_{f,u}, \quad & L(u,v) &= \mathbf{x}_{f,uu}\mathbf{n}, \\ F(u,v) &= \mathbf{x}_{f,u}\mathbf{x}_{f,v}, \quad & M(u,v) &= \mathbf{x}_{f,uv}\mathbf{n}, \\ G(u,v) &= \mathbf{x}_{f,v}\mathbf{x}_{f,v}, \quad & N(u,v) &= \mathbf{x}_{f,vv}\mathbf{n}, \end{aligned} \tag{A3}$$

where the subscripts u and v stand for the partial derivative with respect to them, and $\mathbf{n}(u,v)$ is a unit vector normal to the surface defined as

$$\mathbf{n}(u,v)=\frac{\mathbf{x}_{f,u}\times\mathbf{x}_{f,v}}{|\mathbf{x}_{f,u}\times\mathbf{x}_{f,v}|}. \tag{A4}$$

Since we take $u=\text{const}$ and $v=\text{const}$ as the lines of curvature, we obtain

$$F(u,v)=M(u,v)=0. \tag{A5}$$

We define the third coordinate w [31] by

$$\mathbf{x}(u,v,w)=\mathbf{x}_f(u,v)+w\mathbf{n}(u,v), \tag{A6}$$

taking w positive (negative) for the outside (inside) of the F ball. We take $w=0$ at the place in the wall where the scalar field ϕ vanishes.

Using the orthogonal relations

$$\mathbf{x}_{f,u}\mathbf{x}_{f,v}=\mathbf{x}_{f,u}\mathbf{n}=\mathbf{x}_{f,v}\mathbf{n}=\mathbf{n}\mathrm{d}\mathbf{n}=0, \tag{A7}$$

we express the line element squared,

$$\begin{aligned}\mathrm{d}^2\mathbf{x}&=(\mathbf{x}_{f,u}\mathrm{d}u+\mathbf{x}_{f,v}\mathrm{d}v+\mathbf{n}\mathrm{d}w+w\mathrm{d}\mathbf{n})^2\\&=E\mathrm{d}u^2+G\mathrm{d}v^2+2w(\mathbf{x}_{f,u}\mathrm{d}\mathbf{n}\mathrm{d}u+\mathbf{x}_{f,v}\mathrm{d}\mathbf{n}\mathrm{d}v)\\&\quad+w^2\mathrm{d}\mathbf{n}^2+\mathrm{d}w^2.\end{aligned} \tag{A8}$$

From Eq. (A7) and $M(u,v)=0$ in Eq. (A5), we obtain

$$\mathbf{n}_u=-\frac{L}{E}\mathbf{x}_{f,u}, \tag{A9}$$

$$\mathbf{n}_v=-\frac{N}{G}\mathbf{x}_{f,v}. \tag{A10}$$

Thus, we obtain

$$\mathbf{x}_{f,u}\mathrm{d}\mathbf{n}=\mathbf{x}_{f,u}(\mathbf{n}_u\mathrm{d}u+\mathbf{n}_v\mathrm{d}v)=-L\mathrm{d}u, \tag{A11}$$

$$\mathbf{x}_{f,v}\mathrm{d}\mathbf{n}=\mathbf{x}_{f,v}(\mathbf{n}_u\mathrm{d}u+\mathbf{n}_v\mathrm{d}v)=-N\mathrm{d}v, \tag{A12}$$

$$\mathrm{d}\mathbf{n}^2=(\mathbf{n}_u\mathrm{d}u+\mathbf{n}_v\mathrm{d}v)^2=\frac{L^2}{E}\mathrm{d}u^2+\frac{N^2}{G}\mathrm{d}v^2. \tag{A13}$$

Substituting Eqs. (A11) to (A13) into Eq. (A8), we get

$$\mathrm{d}^2\mathbf{x}=E\left(1-\frac{wL}{E}\right)^2\mathrm{d}u^2+G\left(1-\frac{wN}{G}\right)^2\mathrm{d}v^2+\mathrm{d}w^2. \tag{A14}$$

Calculating a determinant of the line element squared, we obtain the volume element

$$\begin{aligned}\mathrm{d}^3\mathbf{x}&=\sqrt{EG\left(1-\frac{wL}{E}\right)^2\left(1-\frac{wN}{G}\right)^2}\,\mathrm{d}u\mathrm{d}v\mathrm{d}w\\&=\left|\left(1-\frac{wL}{E}\right)\left(1-\frac{wN}{G}\right)\right|\mathrm{d}S\mathrm{d}w,\end{aligned} \tag{A15}$$

where we use the relation

$$\mathrm{d}S=\sqrt{EG}\,\mathrm{d}u\mathrm{d}v. \tag{A16}$$

Taking R_1 and R_2 as the radii of principal curvature of the surface, we obtain the Gaussian curvature

$$K\equiv\frac{1}{R_1R_2}=\frac{LN}{EG}, \tag{A17}$$

the mean curvature

$$H\equiv\frac{1}{2}\left(\frac{1}{R_1}+\frac{1}{R_2}\right)=-\frac{EN+GL}{2EG}, \tag{A18}$$

and the volume element

$$\mathrm{d}^3\mathbf{x}=\left|\left(1+\frac{w}{R_1}\right)\left(1+\frac{w}{R_2}\right)\right|\mathrm{d}S\mathrm{d}w. \tag{A19}$$

APPENDIX B: CURVATURE EFFECT IN THE NEUTRAL CASE

We here derive Eqs. (21)–(24) in Sec. II, assuming R_1, $R_2>0$. Noting that higher order effects in E_{tot} arise only from E_s, we estimate E_s keeping the terms up to the order of $(\delta_n/R)^2$. Substituting Eq. (18) into Eq. (7), we obtain

$$E_s=E_s^{(0)}+E_s^{(1)}+E_s^{(2)}, \tag{B1}$$

where

$$E_s^{(0)}=\int \mathrm{d}S\int_{-\infty}^{+\infty}\mathrm{d}w\ \left\{\frac{1}{2}\dot{\phi}_0{}^2+\frac{\lambda}{8}(\phi_0^2-v^2)^2\right\}, \tag{B2}$$

$$\begin{aligned}E_s^{(1)}=\int \mathrm{d}S\int_{-\infty}^{+\infty}\mathrm{d}w\ &\left[\left(\frac{w}{R_1}+\frac{w}{R_2}\right)\left\{\frac{1}{2}\dot{\phi}_0{}^2+\frac{\lambda}{8}(\phi_0^2-v^2)^2\right\}\right.\\&\left.+\left\{\dot{\phi}_0\dot{\phi}_1+\frac{\lambda}{2}\phi_0(\phi_0^2-v^2)\phi_1\right\}\right],\end{aligned} \tag{B3}$$

$$\begin{aligned}E_s^{(2)}=\int \mathrm{d}S\int_{-\infty}^{+\infty}\mathrm{d}w\ &\left[\frac{w^2}{R_1R_2}\left\{\frac{1}{2}\dot{\phi}_0{}^2+\frac{\lambda}{8}(\phi_0^2-v^2)^2\right\}\right.\\&+\left(\frac{w}{R_1}+\frac{w}{R_2}\right)\left\{\dot{\phi}_0\dot{\phi}_1+\frac{\lambda}{2}\phi_0(\phi_0^2-v^2)\phi_1\right\}\\&\left.+\left\{\frac{1}{2}\dot{\phi}_1{}^2+\frac{\lambda}{4}(3\phi_0^2-v^2)\phi_1^2\right\}\right].\end{aligned} \tag{B4}$$

Substituting Eq. (15) into Eq. (B2), we get

$$E_s^{(0)}=\Sigma\int \mathrm{d}S, \tag{B5}$$

with $\Sigma=2\sqrt{\lambda}v^3/3$. The integration of Eq. (B3) vanishes:

$$E_s^{(1)}=0, \tag{B6}$$

because the integrand is an odd function of w. Using the relation, $\dot{\phi}_0{}^2=\lambda(\phi_0^2-v^2)^2/4$ derived from Eq. (13), we express the first line in the right-hand side of Eq. (B4) as

$$(\text{1st line})=\int dS\int_{-\infty}^{+\infty}dw\;\frac{w^2}{R_1R_2}\dot{\phi}_0{}^2. \tag{B7}$$

The second line is rewritten as

$$(\text{2nd line})=\int dS\int_{-\infty}^{+\infty}dw\;\left[\left(\frac{w}{R_1}+\frac{w}{R_2}\right)\left\{-\ddot{\phi}_0+\frac{\lambda}{2}\times\phi_0(\phi_0^2-v^2)\right\}\phi_1-\left(\frac{1}{R_1}+\frac{1}{R_2}\right)\dot{\phi}_0\phi_1\right]$$
$$=-\int dS\int_{-\infty}^{+\infty}dw\;\left(\frac{1}{R_1}+\frac{1}{R_2}\right)\dot{\phi}_0\phi_1. \tag{B8}$$

From Eq. (19), we get for the third line,

$$(\text{3rd line})=\int dS\int_{-\infty}^{+\infty}dw\;\left\{-\frac{1}{2}\ddot{\phi}_1+\frac{\lambda}{4}(3\phi_0^2-v^2)\phi_1\right\}\phi_1$$
$$=\frac{1}{2}\int dS\int_{-\infty}^{+\infty}dw\;\left(\frac{1}{R_1}+\frac{1}{R_2}\right)\dot{\phi}_0\phi_1. \tag{B9}$$

From Eqs. (B7) to (B9), we obtain

$$E_s^{(2)}=\int dS\int_{-\infty}^{+\infty}dw\;\left\{\frac{w^2}{R_1R_2}\dot{\phi}_0{}^2-\frac{1}{2}\left(\frac{1}{R_1}+\frac{1}{R_2}\right)\dot{\phi}_0\phi_1\right\}. \tag{B10}$$

Using the dimensionless quantity

$$\tilde{\phi}_1\equiv\frac{2R_1R_2}{R_1+R_2}\phi_1, \tag{B11}$$

we express $E_s^{(2)}$ as

$$E_s^{(2)}=\int dS\int_{-\infty}^{+\infty}dw\;\left\{\frac{w^2}{R_1R_2}\dot{\phi}_0{}^2-\frac{1}{4}\left(\frac{1}{R_1}+\frac{1}{R_2}\right)^2\dot{\phi}_0\tilde{\phi}_1\right\}$$
$$=C_n\int dS\;\frac{1}{R_1R_2}+D_n\int dS\;\left(\frac{1}{R_1}-\frac{1}{R_2}\right)^2, \tag{B12}$$

with

$$C_n=\int_{-\infty}^{+\infty}dw\;(w^2\dot{\phi}_0{}^2-\dot{\phi}_0\tilde{\phi}_1), \tag{B13}$$

$$D_n=-\frac{1}{4}\int_{-\infty}^{+\infty}dw\,\dot{\phi}_0\tilde{\phi}_1. \tag{B14}$$

From Eq. (19) with Eq. (20), we get

$$\tilde{\phi}_1(w)=\frac{1}{\sqrt{\lambda}}\operatorname{sech}^2\left(\frac{w}{\delta_n}\right)-\frac{1}{\sqrt{\lambda}}\cosh^2\left(\frac{w}{\delta_n}\right)+\frac{1}{3\sqrt{\lambda}}\sinh^2\left(\frac{w}{\delta_n}\right)\tanh^2\left(\frac{w}{\delta_n}\right)+\frac{1}{12\sqrt{\lambda}}\operatorname{sech}^2\left(\frac{w}{\delta_n}\right)$$
$$\times\left|\sinh\left(\frac{4w}{\delta_n}\right)+8\sinh\left(\frac{2w}{\delta_n}\right)+\frac{12w}{\delta_n}\right|, \tag{B15}$$

with $\delta_n=2/\sqrt{\lambda}v$. Substituting Eqs. (15) and (B15) into Eqs. (B13) and (B14), we obtain

$$C_n=\frac{v}{\sqrt{\lambda}}\int_0^{\infty}d\tilde{w}\;\left\{4\tilde{w}^2\operatorname{sech}^4\tilde{w}-2\operatorname{sech}^4\tilde{w}+2-\frac{2}{3}\tanh^4\tilde{w}-\frac{1}{6}\operatorname{sech}^4\tilde{w}(\sinh 4\tilde{w}+8\sinh 2\tilde{w}+12\tilde{w})\right\}$$
$$=\frac{v}{\sqrt{\lambda}}\left(\int_0^{\infty}d\tilde{w}\;\;4\tilde{w}^2\operatorname{sech}^4\tilde{w}-\frac{10}{9}\right)\simeq-\frac{0.25v}{\sqrt{\lambda}}, \tag{B16}$$

$$D_n=\frac{v}{\sqrt{\lambda}}\int_0^{\infty}d\tilde{w}\;\left\{-\frac{1}{2}\operatorname{sech}^4\tilde{w}+\frac{1}{2}-\frac{1}{6}\tanh^4\tilde{w}-\frac{1}{24}\operatorname{sech}^4\tilde{w}(\sinh 4\tilde{w}+8\sinh 2\tilde{w}+12\tilde{w})\right\}$$
$$=-\frac{5v}{18\sqrt{\lambda}}. \tag{B17}$$

APPENDIX C: ENERGY OF AN UNSCREENED *F* BALL

We derive the thin-wall representations for the energy of an unscreened charged *F* ball, Eqs. (31), (32), and (33). We first consider the surface energy

$$E_s=\Sigma\int dS. \tag{C1}$$

Using Eq. (26), we get the metric of the surface,

$$d\mathbf{x}^2=(r^2+\dot{r}^2)d\theta^2+r^2\sin^2\theta d\varphi^2, \tag{C2}$$

with the overdot symbol standing for the derivative with respect to θ. From Eq. (C2), we obtain

$$dS=r^2\sqrt{1+\left(\frac{\dot{r}}{r}\right)^2}\,d\Omega. \tag{C3}$$

Substituting dS in Eq. (C3) into Eq. (C1), with r expressed in Eq. (28), and using the following orthogonality relations:

$$\int\frac{d\Omega}{4\pi}P_lP_m=\frac{1}{2l+1}\delta_{lm}, \tag{C4}$$

$$\int\frac{d\Omega}{4\pi}\dot{P}_l\dot{P}_m=\frac{l(l+1)}{2l+1}\delta_{lm}, \tag{C5}$$

we obtain Eq. (31) with Eq. (34).

We next consider the Fermi energy,

$$E_f=\frac{4\sqrt{\pi}}{3}\int \mathrm{d}S \quad \sigma_f^{3/2}. \tag{C6}$$

Using Eq. (30) and Eq. (C3), we rewrite Eq. (C6) as

$$\begin{aligned} E_f&=\frac{2N_f^{3/2}}{3R}\int \frac{\mathrm{d}\Omega}{4\pi}\frac{(1+\delta\sigma_f)^{3/2}}{(1+\delta S)^{1/2}} \\ &=\frac{2N_F^{3/2}}{3R}\int \frac{\mathrm{d}\Omega}{4\pi}(1+\delta F), \end{aligned} \tag{C7}$$

where

$$\delta F=\frac{3}{2}\delta\sigma_f+\frac{3}{8}\delta\sigma_f^2-\delta r+\delta r^2-\frac{1}{4}\delta\dot{r}^2-\delta\sigma_f\delta r. \tag{C8}$$

This gives Eq. (32) with Eq. (35).

We finally consider the Coulomb energy,

$$E_c=\frac{e^2}{8\pi}\int\int \mathrm{d}S\mathrm{d}S' \ \frac{\sigma_f\sigma_f'}{|\mathbf{x}-\mathbf{x}'|}. \tag{C9}$$

Using the expression

$$\frac{1}{4\pi|\mathbf{x}-\mathbf{x}'|}=\int \frac{\mathrm{d}^3\mathbf{k}}{(2\pi)^3k^2}e^{i\mathbf{k}(\mathbf{x}-\mathbf{x}')}, \tag{C10}$$

we rewrite Eq. (C9) as

$$E_c=\frac{e^2N_F^2}{4\pi^2}\int_0^\infty \mathrm{d}k\int \frac{\mathrm{d}\Omega_k}{4\pi}\left|\int \frac{\mathrm{d}\Omega_x}{4\pi} \ (1+\delta\sigma_f)e^{i\mathbf{kx}}\right|^2. \tag{C11}$$

Using the following expansion relation:

$$\begin{aligned} e^{i\mathbf{kx}}&=\sum_{l=0}^{\infty} i^l j_l(kr)(2l+1)P_l(\cos\Theta_{kx}) \\ &=\sum_{l=0}^{\infty}\sum_m 4\pi i^l j_l(kr)Y_{lm}(\Omega_k)Y_{lm}^*(\Omega_x) \end{aligned} \tag{C12}$$

[here $j_l(kr)$ and $Y_{lm}(\Omega)$ are the spherical Bessel function and the spherical harmonics, respectively, and Θ_{kx} is the angle between $\mathbf{k}$ and $\mathbf{x}$], and the orthogonality relation

$$\int \mathrm{d}\Omega_k Y_{lm}(\Omega_k)Y_{l'm'}^*(\Omega_k)=\delta_{ll'}\delta_{mm'}, \tag{C13}$$

we obtain

$$E_c=\frac{e^2N_F^2}{4\pi^2}\sum_{l=0}^{\infty}\frac{D_c^{(l)}}{2l+1}, \tag{C14}$$

where

$$\begin{aligned} D_c^{(l)}=&(2l+1)^2\lim_{\epsilon\to 0}\int_0^\infty \mathrm{d}k e^{-\epsilon k}\int \frac{\mathrm{d}(\cos\theta)}{2}\sigma_f \\ &\times\int \frac{\mathrm{d}(\cos\theta')}{2}\sigma_f' j_l(kr)j_l(kr')P_l(\cos\theta)P_l(\cos\theta'). \end{aligned} \tag{C15}$$

Here, we have introduced the procedure, $\lim_{\epsilon\to 0}$, in order to safely expand the spherical Bessel function in the integrand,

$$j_l(kr)\simeq j_l(kR)+\delta r kR j_l'(kR)+\frac{1}{2}\delta r^2(kR)^2 j_l''(kR). \tag{C16}$$

Keeping the terms up to the second order, we obtain

$$\begin{aligned} D_c^{(l)}=&(2l+1)^2\lim_{\epsilon\to 0}\int_0^\infty \mathrm{d}k e^{-\epsilon k}\int \frac{\mathrm{d}(\cos\theta)}{2}P_l(\cos\theta) \\ &\times\int \frac{\mathrm{d}(\cos\theta')}{2}P_l(\cos\theta')I_1^{(l)}(\theta,\theta'), \end{aligned} \tag{C17}$$

where

$$\begin{aligned} I_1^{(l)}=&(1+\delta\sigma_f+\delta\sigma_f'+\delta\sigma_f\delta\sigma_f')j_l(kR)^2+(1+\delta\sigma_f+\delta\sigma_f') \\ &\times(\delta r+\delta r')kR j_l(kR)j_l'(kR)+\delta r\,\delta r'(kR)^2[j_l'(kR)]^2 \\ &+\delta r\,\delta r'(kR)^2[j_l'(kR)]^2+\frac{1}{2}(\delta r^2+\delta r'^2) \\ &\times(kR)^2 j_l(kR)j_l''(kR). \end{aligned} \tag{C18}$$

Integrating Eq. (C17) with respect to the angular variables, we get

$$D_c^{(l)}=\lim_{\epsilon\to 0}\int_0^\infty \mathrm{d}k e^{-\epsilon k}I_2^{(l)}, \tag{C19}$$

where

$$\begin{aligned} I_2^{(l)}=&(\delta_{l0}+c_l^2)[j_l(kR)]^2+\left(2\delta_{l0}\sum_{n=1}^{\infty}\frac{a_nc_n}{2n+1}+2a_lc_l\right) \\ &\times kR j_l(kR)J_l'(kR)+a_l^2(kR)^2[j_l'(kR)]^2 \\ &+\delta_{l0}\sum_{n=1}^{\infty}\frac{a_n^2}{2n+1}(kR)^2 j_0(kR)j_0''(kR). \end{aligned} \tag{C20}$$

Using the following integration formulas:

$$\int_0^\infty \mathrm{d}k e^{-\epsilon k}[j_l(kR)]^2=\frac{\pi}{2(2l+1)R}+O(\epsilon), \tag{C21}$$

$$\int_0^\infty \mathrm{d}k e^{-\epsilon k}kR j_l(kR)j_l'(kR)=-\frac{\pi}{4(2l+1)R}+O(\epsilon), \tag{C22}$$

$$\int_0^\infty dk e^{-\epsilon k}(kR)^2[j_l'(kR)]^2=\frac{1}{2\epsilon}-\frac{\pi l(l+1)}{2(2l+1)R}+O(\epsilon,\ \text{or}\ \epsilon\ \log\epsilon), \tag{C23}$$

$$\int_0^\infty dk e^{-\epsilon k}(kR)^2 j_0(kR)j_0''(kR)=-\frac{1}{2\epsilon}+\frac{\pi}{2R}+O(\epsilon,\ \text{or}\ \epsilon\ \log\epsilon), \tag{C24}$$

we obtain Eq. (33) with Eq. (36).

APPENDIX D: DECAY RATE OF AN UNSCREENED *F* BALL

Unscreened charged *F* balls are metastable and fragment through the quantum tunneling (see Sec. III for the details). Here, we roughly estimate the rate of fragmentation, assuming a very simplified model of fragmentation after the ellipsoidal deformation from the spherical shape [32].

We express the surface of the ellipsoidal *F* ball as

$$\frac{x^2}{R^2}+\frac{y^2}{R^2}+\frac{z^2}{R^2\eta^2}=1, \tag{D1}$$

with η being a constant which we call "deformation parameter." Note that R depends on η since it is determined as to minimize the energy of the *F* ball. The surface is also expressed in the polar coordinates as

$$r=R_f(\theta)=\frac{\eta R}{\sqrt{\cos^2\theta+\eta^2\sin^2\theta}}. \tag{D2}$$

The scalar field $\phi(r,\theta)$ should satisfy the Euler-Lagrange equation to be derived from Eq. (3),

$$\nabla^2\phi=\phi''+\frac{2}{r}\phi'+\frac{1}{r^2}\ddot{\phi}+\frac{1}{r^2\tan\theta}\dot{\phi}=\frac{\lambda}{2}\phi(\phi^2-v^2), \tag{D3}$$

with the prime and overdots, standing for $\partial/\partial r$ and $\partial/\partial\theta$, respectively. Here, the boundary conditions are imposed,

$$\phi(r\to\infty)=+v,$$
$$\phi(r=R_f)=0, \tag{D4}$$
$$\phi(r\to 0)\sim -v.$$

(The last one becomes exact when R_f tends to infinity [see Eq. (D7)].) Using the following variable:

$$\tilde{r}=r-R_f(\theta), \tag{D5}$$

and keeping the terms of the leading order for $R_f\to\infty$, we can rewrite Eq. (D3) as

$$\frac{1}{\Theta^2}\frac{\partial^2\phi}{\partial\tilde{r}^2}=\frac{\lambda}{2}\phi(\phi^2-v^2), \tag{D6}$$

to give the solution

$$\phi=v\tanh\left\{\Theta\frac{(r-R_f)}{\delta_n}\right\}, \tag{D7}$$

with $\delta_n=2/\sqrt{\lambda}v$ and

$$\Theta=\frac{1}{\sqrt{1+\frac{1}{R_f^2}\left(\frac{\partial R_f}{\partial\theta}\right)^2}} \tag{D8}$$

$$=\frac{\cos\theta^2+\eta^2\sin\theta^2}{\sqrt{\cos\theta^2+\eta^4\sin\theta^2}}. \tag{D9}$$

We regard the deformation parameter η as the time-dependent dynamical variable. Substituting ϕ into the Lagrangian density of Eq. (3) with the Fermi, the Coulomb, and the volume effect added to it, and integrating it over the whole space, we get the Lagrangian

$$L=\frac{1}{2}h(\eta)\dot{\eta}^2-W(\eta), \tag{D10}$$

where $h(\eta)$ and $W(\eta)$ are estimated as follows. First, $h(\eta)$ is expressed as

$$h(\eta)=2\pi v^2\int\int dr d\theta r^2\sin\theta\left(\frac{\frac{\partial}{\partial\eta}\left\{\Theta\frac{(r-R_f)}{\delta_n}\right\}}{\cosh^2\left\{\Theta\frac{(r-R_f)}{\delta_n}\right\}}\right)^2 \tag{D11}$$

$$\simeq 4\pi\Sigma R^4\left\{-\frac{\eta^4}{R^2}\left(\frac{\partial R}{\partial\eta}\right)^2 N_1+2\frac{\eta^3}{R}\left(\frac{\partial R}{\partial\eta}\right)N_2-\eta^2N_3\right\}, \tag{D12}$$

where

$$N_k=\int_0^1 dx x^{2(k-1)}\{(\eta^2-1)x^2-\eta^2\}^{-k}\times\{\eta^4-(\eta^4-1)x^2\}^{-1/2}\quad(k=1,2,3). \tag{D13}$$

Since $1/\cosh^4\{\Theta(r-R_f)/\delta_n\}$ in the integrand in Eq. (D11) is negligibly small except at around $r\sim R_f$, we approximate the quantities which are smooth at $r\sim R_f$ to those at $r=R_f$. Now let us estimate $W(\eta)=E_v+E_s+E_f+E_c$. We easily obtain the volume energy

$$E_v=\frac{4\pi R^3\eta}{3}\epsilon. \tag{D14}$$

In order to estimate E_s, E_f, and E_c, we introduce new variables $\hat{\theta}$ and $\hat{\varphi}$ defined by

$$x = R \sin\hat{\theta}\cos\hat{\varphi},$$
$$y = R \sin\hat{\theta}\sin\hat{\varphi}, \tag{D15}$$
$$z = \eta R \cos\hat{\theta}.$$

The surface element is expressed as

$$\begin{aligned} \mathrm{d}S &= R^2\sqrt{\cos^2\hat{\theta} + \eta^2\ \sin^2\ \hat{\theta}}\,\sin\hat{\theta}\mathrm{d}\hat{\theta}\mathrm{d}\hat{\varphi} \\ &= R^2\sqrt{k(u)}\mathrm{d}u\,\mathrm{d}\hat{\varphi}, \end{aligned} \tag{D16}$$

where $u = \cos\hat{\theta}$ and $k(u) = u^2 + \eta^2(1-u^2)$. From Eq. (D16), we obtain the surface energy

$$E_s = \Sigma\int \mathrm{d}S = 4\pi\Sigma R^2\int_0^1 \mathrm{d}u\ \sqrt{k(u)}. \tag{D17}$$

We express the fermion number density,

$$\sigma_f(u) = \frac{N_f}{4\pi R^2\sqrt{k(u)}}\left(1+\sum_{l=1}^{\infty} n_l P_l(u)\right), \tag{D18}$$

where $P_l(u)$ is the lth order Legendre polynomial. It is easy to see that the above expression satisfies the condition for the fermion number N_f to be conserved [see Eq. (8)]. From Eq. (D16) and Eq. (D18), we obtain the Fermi energy,

$$E_f = \frac{4\sqrt{\pi}}{3}\int \mathrm{d}S\ \ \sigma_f^{3/2} = \frac{2N_f^{3/2}}{3R}\int_0^1 \mathrm{d}u\ \frac{\left(1+\sum_{l=1}^{\infty} n_l P_l(u)\right)^{3/2}}{k(u)^{1/4}}. \tag{D19}$$

Let us estimate the Coulomb energy,

$$E_c = \frac{e^2}{8\pi}\int\int \mathrm{d}S\mathrm{d}S'\ \frac{\sigma_f\sigma_f'}{|\mathbf{x}-\mathbf{x}'|}. \tag{D20}$$

Using the relation

$$\begin{aligned} \frac{1}{4\pi|\mathbf{x}-\mathbf{x}'|} &= \int \frac{\mathrm{d}^3\mathbf{q}}{(2\pi)^3 q^2} e^{i\mathbf{q}(\mathbf{x}-\mathbf{x}')} \\ &= \int \frac{\mathrm{d}^3\hat{\mathbf{q}}}{(2\pi)^3\hat{q}^2 k(u_{\hat{q}})} e^{i\hat{\mathbf{q}}(\hat{\mathbf{x}}-\hat{\mathbf{x}}')}, \end{aligned} \tag{D21}$$

with

$$\hat{\mathbf{x}} = \left(x_x, x_y, \frac{1}{\eta}x_z\right) = R(\sin\hat{\theta}\cos\hat{\varphi}, \sin\hat{\theta}\sin\hat{\varphi}, \cos\hat{\theta}), \tag{D22}$$

$$\hat{\mathbf{q}} = (q_x, q_y, \eta q_z), \tag{D23}$$

and $u_{\hat{q}} = \hat{q}_z/\hat{q}$, we get

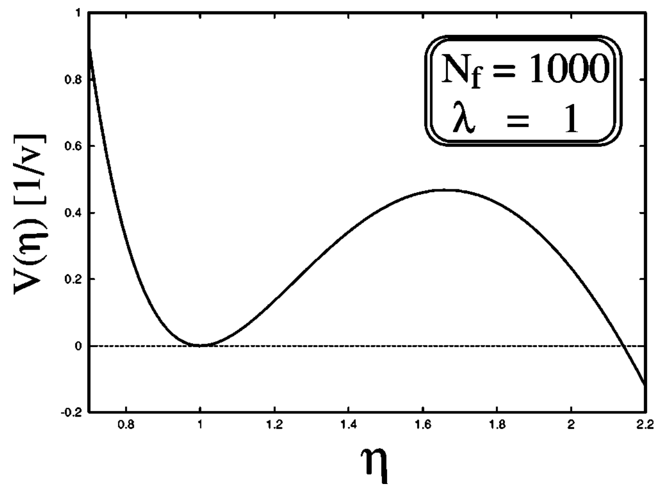

FIG. 6. The potential is displayed as a function of η in case the F ball is not screened for the parameters shown in the graph. There is an energy barrier, which is comparable to v. The distribution of the fermion is shown in Fig. 7.

$$\begin{aligned} E_c = \frac{e^2 N_f^2 \eta}{4\pi^2}\int_0^{\infty}\mathrm{d}\hat{q}\int \frac{\mathrm{d}\Omega_{\hat{q}}}{4\pi k(u_q)} \\ \times\left|\int \frac{\mathrm{d}\Omega_{\hat{x}}}{4\pi}\left(1+\sum_{l=1}^{\infty} n_l P_l(u)\right) e^{i\hat{\mathbf{q}}\hat{\mathbf{x}}}\right|^2. \end{aligned} \tag{D24}$$

With the aid of

$$\begin{aligned} \int_0^{\infty}\mathrm{d}q\, j_l(qR) j_{l'}(qR) = \frac{\pi}{2(2l+1)R}\delta_{ll'} \quad \text{for } l-l' \\ = \text{even integer}, \end{aligned} \tag{D25}$$

the integration in Eq. (D24) can be carried out in the same way as in Appendix C, to give

$$E_c = \frac{e^2 N_f^2}{8\pi R}\int_0^1 \mathrm{d}u\ \frac{\eta}{k(u)}\left(1+\sum_{l=1}^{\infty}\frac{n_l^2 P_l(u)^2}{2l+1}\right). \tag{D26}$$

We then minimize $W(\eta)$ with respect to R and n_l. As expected from the perturbative analysis in Sec. III, we verify numerically that $W(\eta)$ takes the local minimum value W_{min} at $\eta=1$ in a certain range of the parameters (see Fig. 6 for the case, $\epsilon=0$, $\lambda=1$, and $N_f=1000$). In the following, we consider such an F ball which has the local minimum value of W at $\eta=1$, that is, is stable against the deformation from the spherical shape.

We finally proceed to estimate the decay rate of the metastable F ball, using the Euclidean action method in Ref. [33]. We express the Euclidean action as

$$\mathcal{A} = \int \mathrm{d}t\ \left\{\frac{1}{2}h(\eta)\dot{\eta}^2 + V(\eta)\right\}, \tag{D27}$$

where $V(\eta) = W(\eta) - W_{min}$ [we note $V(1)=0$]. Defining the following variable:

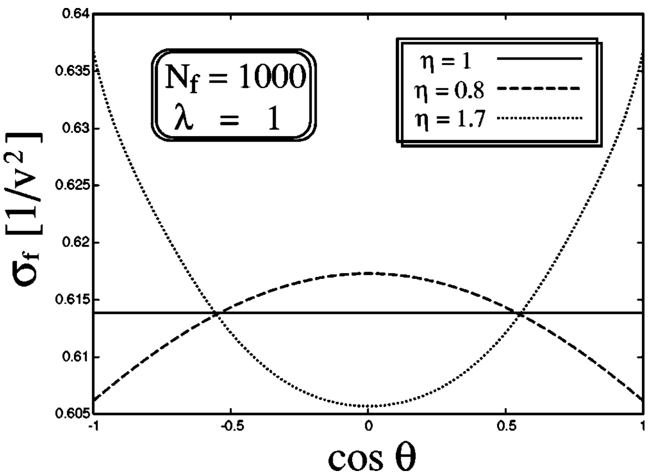

FIG. 7. The number density of the heavy fermion as a function of θ for $\eta=0.8,1,1.7$. The density is constant for $\eta=1$. It gets large at the equator for $\eta=0.8$ and at poles for $\eta=1.7$. They are graphically displayed in Fig. 8.

$$\xi=\int_1^{\eta} d\eta' \sqrt{h(\eta')}, \tag{D28}$$

we express the action as

$$\mathcal{A}=\int dt \left\{\frac{1}{2}\dot{\xi}^2+\bar{V}(\xi)\right\}, \tag{D29}$$

where the potential $\bar{V}(\xi)=V(\eta(\xi))$ has a local minimum $\bar{V}=0$ at $\xi=0$. According to Ref. [33], the decay rate Γ is estimated semiclassically,

$$\Gamma=\hbar|K|e^{-\mathcal{A}_0/\hbar}, \tag{D30}$$

where $\mathcal{A}_0$ is the classical action of the bounce solution and K is the prefactor, both of which are evaluated below. The bounce solution for ξ should satisfy the following equation:

$$\frac{\delta\mathcal{A}}{\delta\xi}=-\ddot{\xi}+\bar{V}'(\xi)=0, \tag{D31}$$

with the boundary condition,

$$\xi\to 0 \quad \text{for } t\to\pm\infty. \tag{D32}$$

From Eq. (D31), we get $\dot{\xi}^2=2\bar{V}(\xi)$ for the classical solution and obtain the classical Euclidean action

$$\mathcal{A}_0=2\int_0^{\xi_c} d\xi \sqrt{2\bar{V}(\xi)}=2\int_1^{\eta_c} d\eta \sqrt{2h(\eta)V(\eta)}, \tag{D33}$$

where $\eta_c(\eta_c>1)$ and $\xi_c(\xi_c>0)$ are defined as $V(\eta_c)=\bar{V}(\xi_c)=0$. The constant K is defined as

$$K=\sqrt{\frac{\mathcal{A}_0}{2\pi\hbar}}\left\{\frac{\det\left(-\frac{\partial^2}{\partial t^2}+\bar{V}''(0)\right)}{\det'\left(-\frac{\partial^2}{\partial t^2}+\bar{V}''(\xi)\right)}\right\}^{1/2}, \tag{D34}$$

where the symbol "det′" means the determinant in which the zero-mode contribution is removed [33]. In our case, K is calculated as

$$\begin{aligned} K&=\sqrt{\frac{\pi}{\hbar}}(\bar{V}''(0))^{3/4}\xi_c \exp\int_0^{\xi_c} d\xi \frac{\sqrt{\bar{V}''(0)}\xi-\sqrt{2\bar{V}(\xi)}}{\xi\sqrt{2\bar{V}(\xi)}} \\ &=\sqrt{\frac{\pi}{\hbar}}\left(\frac{V''(1)}{h(1)}\right)^{3/4}\left(\int_1^{\eta_c} d\eta\sqrt{h(\eta)}\right)\exp\int_1^{\eta_c} d\eta\sqrt{h(\eta)} \\ &\quad\times\left\{\left(\frac{V''(1)}{2h(1)V(\eta)}\right)^{1/2}-\frac{1}{\int_1^{\eta} d\eta'\sqrt{h(\eta')}}\right\}. \end{aligned} \tag{D35}$$

Taking parameters $v=10^5$ GeV, $N_f=1000$, and $\lambda=1$ for example, we obtain $\mathcal{A}_0\simeq 550$. Thus, the lifetime of the unscreened charged F ball is much longer than the age of the universe in this case. (If the production temperature of the F ball T_f is as high as $T_f\sim T_{ph}\sim v$, the F ball would decay through the thermal fluctuation. We here consider the temperature $T_f\lesssim 0.1v\ll T_{ph}$ where the lifetime of the F ball is found to be long enough to let it survive till present.)

APPENDIX E: DECAY RATE OF A SCREENED *F* BALL

Here, we roughly estimate the decay rate of the screened F ball, assuming the very simplified model, in which the surface has the following shape:

$$R_f=R_0[1+a_2P_2(\cos\theta)], \tag{E1}$$

where P_2 is the second order Legendre polynomial and R_0 and a_2 are arbitrary constants. This allows the F ball to have a concave shape. In the following we consider the F ball energy as the function of the area S and the parameter a_2. Then, the parameter R_0 is a function of S and a_2. We use the same technique as that in Appendix D. We here regard a_2 as the time-dependent dynamical variable instead of η in Appendix D. All we need to obtain are $\tilde{h}(a_2)$ and $\tilde{V}(a_2)$ in the Lagrangian,

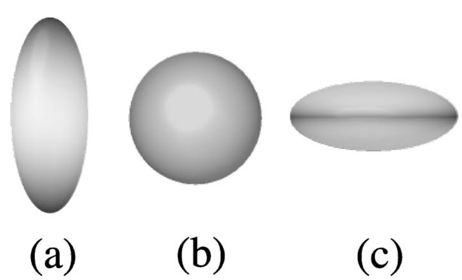

FIG. 8. The distribution of the heavy fermions in case the F ball is not screened. (a) The F ball becomes cigarlike shape for $\eta>1$ and the fermions gather at poles due to the repulsive electric force. (b) The F ball is a sphere for $\eta=1$ and the distribution is constant. (c) The F ball has the pancakelike shape for $\eta<1$, and the fermions gather at the equator due to the repulsive force.

$$L=\frac{1}{2}\tilde{h}(a_2)\dot{a}_2{}^2-\tilde{V}(a_2). \tag{E2}$$

We can easily obtain $\tilde{h}(a_2)$ by replacing R_f in Eqs. (D8) and (D11) with that defined by Eq. (E1).

The potential $\tilde{V}(a_2)$ can be obtained from Eq. (65) since $F_{tot}^{(0)}$ depends only on S and not on the shape of the F ball. We calculate the following quantities using the method introduced in Appendix A:

$$X_C\equiv\int dS\ \frac{1}{|R_1R_2|}, \tag{E3}$$

$$X_D\equiv\int dS\ \left(\frac{1}{R_1}-\frac{1}{R_2}\right)^2\frac{|R_1R_2|}{R_1R_2}. \tag{E4}$$

The surface is expressed as

$$\mathbf{x}=\mathbf{x}_f(\theta,\varphi)=R_f(\theta)(\sin\theta\cos\varphi,\sin\theta\sin\varphi,\cos\theta) \tag{E5}$$

in the polar coordinates. The first and the second forms are

$$I=E(\theta,\phi)d\theta^2+2F(\theta,\phi)d\theta d\phi+G(\theta,\phi)d\phi^2, \tag{E6}$$

$$J=L(\theta,\phi)d\theta^2+2M(\theta,\phi)d\theta d\phi+N(\theta,\phi)d\phi^2, \tag{E7}$$

with

$$\begin{aligned}
E(\theta,\phi)&=R_f^2+R_f'^2,\\
L(\theta,\phi)&=\frac{1}{\sqrt{R_f^2+R_f'^2}}(R_f''^2R_f^2-2R_f'^2-R_f^2),\\
F(\theta,\phi)&=0,\quad M(\theta,\phi)=0,\\
G(\theta,\phi)&=R_f^2\ \sin^2\theta,\\
N(\theta,\phi)&=\frac{R_f}{\sqrt{R_f^2+R_f'^2}}\sin\theta(-R_f\ \sin\theta+R_f\ \cos\theta),
\end{aligned} \tag{E8}$$

where the prime denotes the derivative with respect to θ. From these, the Gaussian curvature in Eq. (A17) and the mean curvature in Eq. (A18) are expressed in terms of R_f. We then obtain

$$\frac{1}{R_1R_2}=K=\frac{(R_f'\ \sin\theta-R_f\ \cos\theta)(-R_f''^2R_f^2+2R_f'^2+R_f^2)}{R_f\sin\theta(R_f^2+R_f'^2)^2}, \tag{E9}$$

$$\begin{aligned}
\left(\frac{1}{R_1}-\frac{1}{R_2}\right)^2&=\frac{(EN-GL)^2}{E^2G^2}\\
&=\frac{\{(R_f^2+R_f'^2)(-R_f'\ \sin\theta+R_f\ \cos\theta)+(-R_f''^2R_f^2+2R_f'^2+R_f^2)R_f\ \sin\theta\}^2}{R_f^2\sin^2\theta(R_f^2+R_f'^2)^3}.
\end{aligned} \tag{E10}$$

From these expressions, X_C and X_D are written as

$$X_C=4\pi\int_0^{\pi/2}d\theta\frac{|(R_f'\ \sin\theta-R_f\ \cos\theta)(-R_f''^2R_f^2+2R_f'^2+R_f^2)|}{(R_f^2+R_f'^2)^{3/2}}, \tag{E11}$$

$$X_D=4\pi\int_0^{\pi/2}d\theta\frac{\{(R_f^2+R_f'^2)(-R_f'\ \sin\theta+R_f\ \cos\theta)+(-R_f''^2R_f^2+2R_f'^2+R_f^2)R_f\ \sin\theta\}^2}{R_f\ \sin\theta(R_f^2+R_f'^2)^{5/2}}\frac{|K|}{K}. \tag{E12}$$

We note that these quantities do not explicitly depend on the parameter R_0 or S and only depend on a_2. Using the free energy,

$$F_{tot}^{(2)}(a_2)=(C_n+C_{sc})X_C+(D_n+D_{sc})X_D, \tag{E13}$$

we evaluate the potential

$$\tilde{V}(a_2)=F_{tot}^{(2)}(a_2)-F_{tot}^{(2)}(0). \tag{E14}$$

We show the potential as a function of a_2 in Fig. 9 for the case $T=0.1v$. The cusp in Fig. 9 arises because of the nonanalytic feature of X_C and X_D. At the top of the cusp, the Gaussian curvature becomes zero at equator and turns to be negative for larger a_2. This is illustrated in Fig. 10. One can

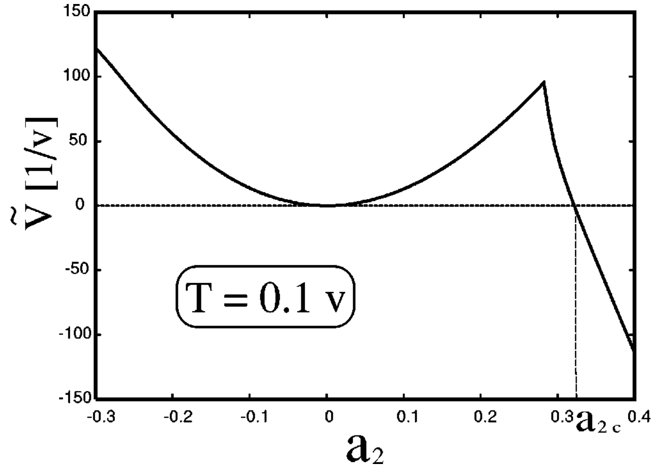

FIG. 9. The potential of the screened F ball as a function of a_2. The curvature at the origin is positive and the potential becomes negative for a_2 larger than a_{2c} at $T=0.1v$. These facts mean that the spherical F ball ($a_2=0$) is metastable. The energy barrier is much larger than the temperature. This tells us that the decay due to the thermal fluctuation can be neglected.

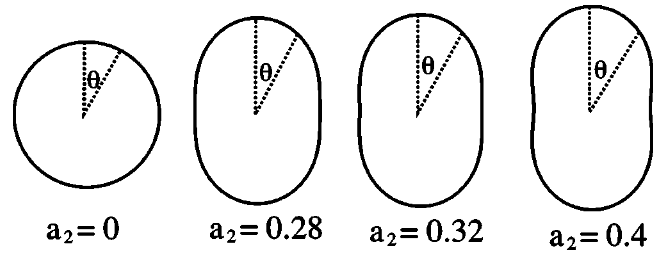

FIG. 10. The shapes of the F ball for various values of the parameter a_2. A geometrical cross section containing z axis is shown. The shape is a sphere for $a_2=0$. One of the principal radii is divergent at the equator for $a_2=2/7\sim 0.28$ in which the potential has the crest. The shape becomes slightly nonconvex at the equator for $a_2=a_{2c}\sim 0.32$ and more narrow in the middle for $a_2=0.4$.

observe that the curvature at the origin is positive and the potential becomes negative for a_2 larger than a_{2c}. These facts mean that the spherical F ball is metastable as discussed in Sec. IV. Because the energy barrier is much larger than the temperature, the decay of the F ball due to thermal fluctuation can be neglected. We next consider the decay due to the tunneling effect.

We consider the classical Euclidean action,

$$\tilde{\mathcal{A}}_0=2\int_0^{a_{2c}} da_2\ \sqrt{2\tilde{h}(a_2)\tilde{V}(a_2)}. \tag{E15}$$

We can apply Eq. (D11) to obtain $\tilde{h}(a_2)$ and see its magnitude is $O(\Sigma R^4)$. We find that the barrier height is $O(100v)$ and a_{2c} is $O(1)$ from Fig. 9. From these, the classical Euclidean action is roughly estimated as $\tilde{\mathcal{A}}_0 \gtrsim N_f$. Since the number of the heavy fermion is large, $N_f > 10^{19}$, from Eqs. (69) and (71), the classical Euclidean action is extremely large and the screened F ball is effectively stable. Although we use the very simple deformation model and take the special case of $T=0.1v$, we think that the result of a very long lifetime is rather general for the temperature smaller than v since the result is only due to the macroscopic property of the F ball.

[1] A.L. Macpherson and B.A. Campbell, Phys. Lett. B **347**, 205 (1995).
[2] J.R. Morris, Phys. Rev. D **59**, 023513 (1999).
[3] R. Brandenberger, I. Halperin, and A. Zhitnitsky, hep-ph/9903318.
[4] This fragmentation is due to a small volume energy, which exists when the symmetry is biased [1].
[5] When the fermions of the F ball have an electric U(1) charge, hereafter we call such an F ball a (electrically) charged F ball. In the same manner, we define the terminology of the neutral F ball for that Macpherson and Campbell originally introduced.
[6] D.N. Spergel and P.J. Steinhardt, Phys. Rev. Lett. **84**, 3760 (2000).
[7] J.A. Tyson, G.P. Kochanski, and I.P. Dell'antonio, Astrophys. J. Lett. **498**, L107 (1998).
[8] K. Ogure, T. Yoshida, and J. Arafune, KOBE-TH-02-03, hep-ph/0212332.
[9] Note that the qualitative discussions in the following do not depend on the explicit form of $U(\phi)$.
[10] Such zero-mode solutions for ψ_f can also exist in other cases, such as in the context of supersymmetry [34,35].
[11] In our context, we call the plane where the expectation value of ϕ vanishes the "surface of the F ball."
[12] Here R is the order of the curvature radius. Note that the validity of this thin-wall expansion collapses for the small F ball, $N_f\sim 16\pi^{2/3}/\lambda^{2/3}$.
[13] The solution for ϕ_1 is not smooth at $w=0$. This is caused by the Yukawa term $-G\overline{\psi_f}\psi_f\phi$ which is implicit in Eq. (7). Because of the curvature of the surface, $\overline{\psi_f}\psi_f$ does not vanish and is approximately proportional to $\delta(w)$, which is also implicit in the rhs of Eq. (19), giving the discontinuity of $\dot{\phi}_1$ at the F-ball surface in the case where the fermions are tightly bound in the domain wall, $G \gg \sqrt{\lambda}$. If the spreading thickness of the fermions is comparable to the that of the domain wall, the expectation value of the fermions is not like $\delta(w)$. We investigate this case elsewhere [8].
[14] In order to get the order of $(\delta_n/R)^2 E_{tot}^{(0)}$ in E_{tot}, we need only to keep the order of $(\delta_n/R)\phi_0$ in ϕ, as is well known in the perturbation theory.
[15] The integration of the Gaussian curvature on the closed surface takes the topological value, which equals 4π in this case.
[16] J. Arafune, T. Yoshida, S. Nakamura, and K. Ogure, Phys. Rev. D **62**, 105013 (2000).
[17] A.B. Migdal, V.S. Popov, and D.N. Voskresenskii, Zh. Eksp. Teor. Fiz. **72**, 834 (1977).
[18] J.R.S. Nascimento, I. Cho, and A. Vilenkin, Phys. Rev. D **60**, 083505 (1999).
[19] The Thomas-Fermi approximation is adequate for

$|d/dw(1/V_e)| \ll 1$ [18]. We see from Eq. (49) that this condition is satisfied in the region near the surface where most of the electric charge is screened.

[20] J. I. Kapusta, *Finite Temperature Field Theory* (Cambridge University Press, Cambridge, England, 1989).

[21] Note that the validity of the thin-wall expansion collapses for the small F ball, $N_f \sim 7000$.

[22] In general, we cannot factor C_{sc} and D_{sc} out of the integration because they are dependent of σ_f. We see, however, that $\sigma_f = \text{const}$ minimizes $F_{tot}^{(0)}$ and that the deviation from the uniform distribution causes the contributions of the order higher than $(\delta_{sc}/R)^2$ in the thin-wall expansion. Thus, we also take $\sigma_f = \text{const}$ in order to estimate $F_{sc}^{(2)}$.

[23] We define the F ball as being metastable when it is classically stable owing to the energy barrier but decays quantum mechanically with a finite lifetime.

[24] A. Vilenkin and E. P. S. Shellard, *Cosmic String and Other Topological Defects* (Cambridge University Press, Cambridge, 1994).

[25] See, e.g., the textbook E. Kolb and M. S. Turner, *The Early Universe* (Addison-Wesley, Redwood City, CA, 1990).

[26] It is easy to understand within the leading order discussion in the thin-wall expansion [1,2].

[27] A.V. Kravtsov *et al.*, Astrophys. J. **502**, 48 (1998).

[28] M. Oguri, A. Taruya, and Y. Suto, Astrophys. J. **559**, 572 (2001).

[29] R. Dave *et al.*, Astrophys. J. **547**, 574 (2001).

[30] Two lines, $u = \text{const}$ and $v = \text{const}$, are called ''lines of curvature'' if their tangent vectors are parallel to the principal directions.

[31] The coordinates can be defined uniquely as far as two or more normal lines do not intersect. We can neglect the contribution in the energy integration over such a region of intersection, since the region is far from the surface.

[32] The geometrical assumption of an ellipsoidal shape enables us to estimate the upper bound on the lifetime of the F ball.

[33] S. Coleman, *Aspects of Symmetry* (Cambridge University Press, Cambridge, 1985).

[34] J.R. Morris and D. Bazeia, Phys. Rev. D **54**, 5217 (1996).

[35] G. Dvali and M. Shifman, Nucl. Phys. **B504**, 127 (1997); M. Sakamoto and M. Tachibana, Phys. Lett. B **458**, 231 (1999).